

r : remove

e : check english

c : change word

rr : rewrite

Testing quantum decoherence at DUNE

J.A. Carpio,^{1,2} E. Massoni,¹ and A.M. Gago¹

¹Sección Física, Departamento de Ciencias, Pontificia Universidad Católica del Perú, Apartado 1761, Lima, Perú

²Department of Physics, The Pennsylvania State University, University Park, Pennsylvania 16802, USA

We address some theoretical issues of the quantum decoherence phenomenon within the neutrino oscillation framework and carry out various tests under DUNE simulated experimental environment. On the theoretical side, we provide a general expression for an invariant decoherence matrix under a quantum basis rotation. On the simulated experimental side, considering a non-invariant and invariant decoherence matrix, we study the impact on the fitting of the standard oscillation parameters, the sensitivity in the mass hierarchy and CP violation, combining the neutrino and antineutrino mode and all available neutrino oscillation probabilities channels. Furthermore, a sensitivity for the decoherence parameter of order 10^{-24} GeV at 3σ , is obtained for our best case. We also note that a degeneracy between the decoherence parameter and the CP violation phase remains, even though our analysis includes neutrino/antineutrino mode and all probabilities channels.

I. INTRODUCTION

It is well established that neutrino oscillation is induced by non-zero neutrino mass [1–7]. However, the existence of some, still unrevealed, subdominant mechanism is not forbidden. In general, the typical trait of this subleading effects is to the neutrino (oscillation) connection with physics beyond the Standard Model. Within this category there are several theoretical hypothesis such as: neutrino decay [8–33], nonstandard neutrino interactions [34–40], Lorentz and CPT invariance violation [41–47], etc. There is another beyond Standard Model hypothesis which contemplates an interacting environment due to some effects produced either by strings and branes [48, 49] or quantum gravity [50]. The result of the interaction between the neutrino system and the environment is the introduction of decoherence/dissipative parameters into the standard oscillation framework [51, 52]. Although the decoherence phenomenon being applied to a neutrino system has been largely studied in the literature [51–69], there is still room for new contributions. This paper is motivated for two interesting points raised in [67]: the first was the discussion about the invariance of the decoherence matrix when we rotate the neutrino Hamiltonian in matter from the vacuum mass eigenstate basis (VMB) to the matter mass eigenstates basis (MMB). The second was the possibility of having a degeneracy in oscillation probabilities between the decoherence parameter Γ and the CP violation phase δ .

In this paper, we will present a detailed demonstration of the behaviour of the decoherence matrix under rotations and obtain the general shape of a (rotation) invariant decoherence matrix. Furthermore, we will probe the neutrino oscillation probabilities for an invariant and non-invariant decoherence matrix under simulated experimental conditions in the context of DUNE, which will have unprecedented sensitivity to the identification of the mass hierarchy and the measurement of the CP phase δ [70]. Considering the two aforementioned kinds of decoherence matrix, we will perform various tests such as:

the sensitivity to the decoherence parameter, the effects of decoherence in the measurement of oscillation parameters and in the sensitivity to the mass hierarchy and δ . We include, of course, the study of the degeneracy between Γ and δ , in agreement with our second motivation point.

II. THEORETICAL CONSIDERATIONS

A. Density matrix formalism

The description of the neutrino system weakly interacting with the environment using the open quantum system approach is given by:

$$\frac{d\hat{\rho}(t)}{dt} = -i[H, \hat{\rho}(t)] + D[\hat{\rho}(t)] \quad (1)$$

this is the well known Lindblad Master Equation, where $\hat{\rho}(t)$ is the neutrino's density matrix and H is the Hamiltonian of the system. The term D , which is the one that encloses the dissipative/decoherence effects, is written as:

$$D[\hat{\rho}(t)] = \frac{1}{2} \sum_j \left([\hat{V}_j, \hat{\rho}(t) \hat{V}_j^\dagger] + [\hat{V}_j \hat{\rho}(t), \hat{V}_j^\dagger] \right) \quad (2)$$

where $\{\hat{V}_j\}$ is a set of dissipative operators with $j = 1, 2, \dots, 8$ for 3 neutrino generations. The operators $\{\hat{V}_j\}$, $\hat{\rho}$ and H can be expanded in terms of the $SU(3)$ Gell-Mann matrices. After several intermediate manipulations, well explained in [67], we can arrive at the solution of the Lindblad Master Equation:

$$\vec{\rho}(t) = e^{(M_H + M_D)t} \vec{\rho}(0) \quad (3)$$

where $\vec{\rho}$ is an eight-dimensional column vector consisting of the ρ_k , the components of the quoted expansion before, the 8×8 matrices M_H and M_D , are encoding the hamiltonian and decoherence components of the same expansion, respectively. The dissipative/decoherence matrix M_D , that contains all the decoherence parameters, has

to be a symmetric, positive-semidefinite matrix, and its entries should satisfy a set of inequalities (see [71] for a full list).

Thus, we can get the oscillation probabilities $P(\nu_\alpha \rightarrow \nu_\beta) \equiv P_{\nu_\alpha \nu_\beta}$ that can be obtained via inner products

$$P_{\nu_\alpha \nu_\beta} = \frac{1}{3} + \frac{1}{2} \vec{\rho}_{\nu_\beta} \cdot \vec{\rho}_{\nu_\alpha}(t) \quad (4)$$

where $\vec{\rho}_{\nu_\alpha}(t)$ is the time evolved state from an initial neutrino flavour ν_α and $\vec{\rho}_{\nu_\beta}$ is the final neutrino flavour ν_β to be detected. Considering that the neutrinos are ultrarelativistic, we have $t = L$ where L is the baseline.

B. Neutrino Hamiltonian, rotation and CP phase

The neutrino Hamiltonian $\hat{H}_{VAC} + \hat{A}$ in the VMB for a neutrino of energy E_ν is given by:

$$\hat{H} = \hat{H}_{VAC} + \hat{A} \quad H_V(\delta) = \frac{1}{2E_\nu} \left\{ \begin{pmatrix} 0 & 0 & 0 \\ 0 & \Delta m_{21}^2 & 0 \\ 0 & 0 & \Delta m_{31}^2 \end{pmatrix} + U^\dagger \begin{pmatrix} A_{CC} & 0 & 0 \\ 0 & 0 & 0 \\ 0 & 0 & 0 \end{pmatrix} U \right\} \quad (5)$$

where $\hat{H}_{VAC} = \text{Diag}(0, \Delta m_{21}^2/2E_\nu, \Delta m_{31}^2/2E_\nu)$, $\hat{A} = U^\dagger \text{Diag}(A_{CC}/2E_\nu, 0, 0)U$, with $A_{CC} = 2E\sqrt{2}G_F n_e$, where G_F, n_e are the Fermi coupling constant and electron number density, respectively. Being that U is defined as

$$U = U_{23} U_{\delta}^\dagger U_{13} U_{\delta} \quad (6)$$

with $U_\delta = \text{Diag}(1, 1, e^{-i\delta})$ and, considering that, the matrix $U_{23} U_\delta^\dagger$ commutes with $\text{Diag}(A_{CC}, 0, 0)$ and the matrix U_δ commutes with U_{13} and $\text{Diag}(0, \Delta m_{21}^2, \Delta m_{31}^2)$, separately, the neutrino Hamiltonian can be re-written as follows

$$H_V(\delta) = U_\delta^\dagger H_V(0) U_\delta \quad (7)$$

where $H_V(0)$ is given by

$$H_V(0) = \frac{1}{2E_\nu} \left\{ \begin{pmatrix} 0 & 0 & 0 \\ 0 & \Delta m_{21}^2 & 0 \\ 0 & 0 & \Delta m_{31}^2 \end{pmatrix} + U_{12}^\dagger U_{13}^\dagger \begin{pmatrix} A & 0 & 0 \\ 0 & 0 & 0 \\ 0 & 0 & 0 \end{pmatrix} U_{13} U_{12} \right\} \quad (8)$$

The Hamiltonian H_V defined in the VMB can be related with the Hamiltonian \hat{H}_M in the MMB (this is where the Hamiltonian is diagonal) through:

$$\hat{H}_M(\delta) = U_T^\dagger(\delta, \phi_1, \phi_2) H_V(\delta) U_T(\delta, \phi_1, \phi_2) \quad (9)$$

Using Eq. (7) and that $H_M(\delta)$ commutes with the unitary phase operator $U_\phi^\dagger(\phi_1, \phi_2) = \text{Diag}(1, e^{-i\phi_1}, e^{-i\phi_2})$

def. U_T .

being ϕ_1 and ϕ_2 arbitrary phases, the latter equation can be rewritten as follows:

$$H_M(\delta) = U_\phi^\dagger(\phi_1, \phi_2) U_T^\dagger(\delta, \phi_1, \phi_2) U_\delta^\dagger H_V(0) \times U_\delta U_T(\delta, \phi_1, \phi_2) U_\phi(\phi_1, \phi_2) \quad (10)$$

Since $H_M(\delta)$ can be represented by a unitary transformation of the operator $H_V(0)$, the eigenvalues of the former do not depend on δ either. We thus write:

$$H_M(\delta) = H_M(0) = U_T^\dagger(0, 0, 0) H_V(0) U_T(0, 0, 0) \quad (11)$$

Comparing Eqs. (10) and (11) we obtain

$$U_T(\delta, \phi_1, \phi_2) = U_T^\dagger(0, 0, 0) U_\phi^\dagger(\phi_1, \phi_2) \quad (12)$$

This result implies that once we find a matrix $U_T(0, 0, 0)$ that diagonalizes $H_V(0)$, a general $U_T(\delta, \phi_1, \phi_2)$ that diagonalizes $H_V(\delta)$ can be constructed. → ok

C. Invariant matrices analysis

As mentioned in Ref. [67], the relationship between VMB and MMB decoherence matrices goes as follows:

$$M_D^M(\delta, \phi_1, \phi_2) = P^T(\delta, \phi_1, \phi_2) M_D^V P(\delta, \phi_1, \phi_2) \quad (13)$$

being $P(\delta, \phi_1, \phi_2)$ defined as:

$$P(\delta, \phi_1, \phi_2) = R(\delta) P_0 \hat{R}(\phi_1, \phi_2) \quad (14)$$

expressions for way? this important?
where further details about $P_0 = P(0, 0, 0)$, $R(\delta)$, and $\hat{R}(\phi_1, \phi_2)$ are given in the appendix. Although we are emphasizing the dependence of M_D^M on δ and the arbitrary phases ϕ_1 and ϕ_2 in the Eq. (13), it is important to notice that this matrix, in general, may depend on the neutrino energy and the matter potential A . On the other hand, we point out that in our previous work [67], the above relation was written in an opposite way: $M_D^M = P M_D^V P^T$.

We rewrite Eq. (13) more explicitly:

$$M_D^M(\delta, \phi_1, \phi_2) = \hat{R}^T(\phi_1, \phi_2) P_0^T R^T(\delta) M_D^V \times R(\delta) P_0 \hat{R}(\phi_1, \phi_2) \quad (15)$$

and wish to impose the condition $M_D^M = M_D^V$, meaning that the decoherence matrix M_D^V is invariant under rotations in P . This situation is very convenient to deal with since the neutrino matter oscillation plus quantum decoherence probability formulae are easily found from its corresponding formulae in vacuum (see [67]). We want to prove that, given an invariant matrix M_D^V at $\delta = 0$, it is possible to derive invariant matrices \hat{M}_D^V for other δ . We start with the invariance condition $M_D^M(\delta, \phi_1, \phi_2) = M_D^V$ for $\delta = 0$:

$$M_D^V = \hat{R}^T(\phi_1, \phi_2) P_0^T M_D^V P_0 \hat{R}(\phi_1, \phi_2) \quad (16)$$

this is the "definition" of MMB.

For the case $\delta \neq 0$, the invariance condition for \hat{M}_D^V reads:

$$\begin{aligned}\hat{M}_D^V &= \hat{R}^T(\tilde{\phi}_1, \tilde{\phi}_2) P_0^T R^T(\delta) \hat{M}_D^V \\ &\times R(\delta) P_0 \hat{R}(\tilde{\phi}_1, \tilde{\phi}_2).\end{aligned}\quad (17)$$

Applying the following relation to the preceding equation we obtain

$$\hat{M}_D^V = R(\delta) M_D^V R^T(\delta), \quad (18)$$

and

together with Eq.(16) we get:

$$M_D^M(\delta, \tilde{\phi}_1, \tilde{\phi}_2) = \hat{R}^T(\tilde{\phi}_1, \tilde{\phi}_2) \hat{R}(\phi_1, \phi_2) M_D^V \quad (19)$$

$$\times \hat{R}^T(\phi_1, \phi_2) \hat{R}(\tilde{\phi}_1, \tilde{\phi}_2). \quad (20)$$

Thus if we demand $\hat{R}^T(\tilde{\phi}_1, \tilde{\phi}_2) \hat{R}(\phi_1, \phi_2) = R(\delta)$ the condition $M_D^M(\delta, \tilde{\phi}_1, \tilde{\phi}_2) = \hat{M}_D^V$ is achieved and \hat{M}_D^V is invariant.

In Ref. [67], it is found that for $\delta = 0, \pi$ the invariant matrix M_D^V is given by

$$M_D^V = -\text{Diag}(\Gamma_1, \Gamma_2, \Gamma_1, \Gamma_1, \Gamma_2, \Gamma_1, \Gamma_2, \Gamma_1), \quad (21)$$

with $\Gamma_1/3 \leq \Gamma_2 \leq 5\Gamma_1/3$. Substituting this M_D^V into Eq. (18), we can extrapolate that the corresponding invariant \hat{M}_D^V for any δ is described by the following block diagonal matrix.

$$\hat{M}_D^V = R(\delta) M_D^V R^T(\delta) = -\begin{pmatrix} \Gamma_1 & & & & \\ & \Gamma_2 & & & \\ & & \Gamma_1 & & \\ & & & Q & \\ & & & & Q \\ & & & & & \Gamma_1 \end{pmatrix}, \quad (22)$$

where the matrix Q is given by

$$Q = \begin{pmatrix} \Gamma_1 \cos^2 \delta + \Gamma_2 \sin^2 \delta & (\Gamma_1 - \Gamma_2) \cos \delta \sin \delta \\ (\Gamma_1 - \Gamma_2) \cos \delta \sin \delta & \Gamma_2 \cos^2 \delta + \Gamma_1 \sin^2 \delta \end{pmatrix}. \quad (23)$$

From the latter equation we can calculate \hat{M}_D^V for $\delta = \pi/2, 3\pi/2$ getting:

$$\begin{aligned}\hat{M}_D^V &= R(\delta) M_D^V R^T(\delta) \\ &= -\text{Diag}(\Gamma_1, \Gamma_2, \Gamma_1, \Gamma_1, \Gamma_2, \Gamma_1, \Gamma_2, \Gamma_1).\end{aligned}\quad (24)$$

similar to the one mentioned in Ref. [67].

D. Adding Hamiltonian terms in the weak coupling limit

At this point it is interesting to make a comparison between the approach given in [68] for defining invariant matrices, and the one presented here and in [67]. With the purpose of demanding energy conservation, the following conditions are imposed in [68]: $[H_{VAC}, \hat{V}_j] = 0$

and $[\hat{H}_M, \hat{V}_j^M] = 0$, being that \hat{V}_j and \hat{V}_j^M are the dissipator operators written in the VMB (for the pure vacuum case) and in the MMB, respectively. To achieve the aforementioned conditions, it is required that \hat{V}_j changes when the matter potential term \hat{A} is added to the vacuum Hamiltonian H_{VAC} ; all of this in the VMB. The new dissipator operator is defined by: $\hat{V}_j^{\text{new}} = U_T \hat{V}_j U_T^\dagger$, depending on the matter potential and the neutrino energy, in a way that it recovers its vacuum form when it is rotated to the MMB, this is: $\hat{V}_j^M = U_T^\dagger \hat{V}_j^{\text{new}} U_T = U_T^\dagger U_T \hat{V}_j U_T^\dagger U_T = \hat{V}_j$. This situation is incongruent with the underlying regime used for describing the neutrinos as an open quantum system, which is the Born-Markov approximation (BM). The Born approximation is applied when the environment interacts weakly with the neutrino system [72, 73], while the Markovianity assumption implies the use of the Lindblad form (Eq. (2)) [74, 75]. In this evolution, the system is modified by the environment and parameterized by the dissipator operators (i.e. the decoherence matrix), but not viceversa. Thereby, the environment is considered unaffected by the system and the addition of the matter potential term to the vacuum neutrino Hamiltonian should not change (or in a negligible way) the dissipator operator \hat{V}_j .

~~La~~ ~~dissipación~~ este punto es interesante. Discutir más? expandir?

E. Selected decoherence matrix models

For simplicity, ...

Our analysis will be limited to diagonal decoherence matrices due to their relative simplicity. While analytical expressions are available for these matrices in the context of vacuum oscillations [53], oscillations in matter can be found through perturbative expansions. For a generic matrix $M_D^V = -\text{Diag}(\Gamma_1, \Gamma_2, \Gamma_3, \Gamma_4, \Gamma_5, \Gamma_6, \Gamma_7, \Gamma_8)$, we can make an expansion in the small quantities $\alpha = \Delta m_{21}^2 / \Delta m_{31}^2, \theta_{13}$, and $\bar{\Gamma}_i = \Gamma_i L$, assuming the latter is < 0.1 . The lowest order contribution to the transition probability $P_{\nu_\mu \nu_e}$ is found to be

$$\begin{aligned}P_{\nu_\mu \nu_e} &= P_{\nu_\mu \nu_e}^{(0)} + \frac{1}{4} \cos^2 \theta_{23} [\bar{\Gamma}_1 + \bar{\Gamma}_3 + \cos 4\theta_{12} (\bar{\Gamma}_3 - \bar{\Gamma}_1)] \\ &+ \frac{1}{12} (1 - 3 \cos 2\theta_{23}) \bar{\Gamma}_8,\end{aligned}\quad (25)$$

where $P_{\nu_\mu \nu_e}^{(0)}$ is the standard oscillation transition probability. We also notice that only three decoherence parameters of such a matrix dominate the contributions to the probability. Furthermore, these terms do not depend on the neutrino energy or matter potential, leading to a probability shift across all energies - a property that will help us qualitatively explain our results. Using the current values of the standard oscillation(SO) parameters given in Table I, this shift turns out to be positive.

falta
ref. para ref. expatio
los relevantes.

1. Model A

In light of this, the first one-parameter model we propose for this study (referred from now on as model A) assumes $\Gamma_3 = \Gamma_8 = 0$

$$M_D^V = -\text{Diag}(\Gamma, \Gamma, 0, \Gamma/4, \Gamma/4, \Gamma/4, \Gamma/4, 0) \quad (26)$$

Resulting in a
with an approximate expression for the transition probabilities:

$$\begin{aligned} P_{\nu_\mu \nu_e} &= P_{\nu_\mu \nu_e}^{(0)} + \frac{1}{2} \bar{\Gamma} \cos^2 \theta_{23} \sin^2 2\theta_{12} \\ &\quad - \frac{1}{4} \cos^2 \theta_{23} \bar{\Gamma}^2 \left[\sin^4 2\theta_{12} + \sin^2 4\theta_{12} \frac{\sin^2(A\Delta)}{4A^2 \Delta^2} \right] \\ &\quad + \frac{\bar{\Gamma} \theta_{13} \sin 2\theta_{23} \sin 4\theta_{12}}{4(1-A)A\Delta} [\sin(A\Delta) \cos(\delta + A\Delta) \\ &\quad - A^2 \sin \Delta \cos(\delta + \Delta)] \\ &\quad - \frac{\alpha \bar{\Gamma}}{2A^2 \Delta} \cos 2\theta_{12} \cos^2 \theta_{23} \sin^2 2\theta_{12} \\ &\quad \times (\sin 2A\Delta - 2A\Delta). \end{aligned} \quad (27)$$

already defined

In this expression, $\bar{\Gamma} = \Gamma L / \Delta m_{31}^2 L / 4E$ and $A = A_{CC} / \Delta m_{31}^2$. To obtain the antineutrino oscillation probabilities, switch $A \rightarrow -A$ and $\delta \rightarrow -\delta$.

replace

2. Model B

The second model, from now on named model B, is an invariant matrix based on (24), namely

$$M_D^V = -\text{Diag}(\Gamma, 5\Gamma/3, \Gamma, \Gamma, 5\Gamma/3, \Gamma, 5\Gamma/3, \Gamma). \quad (28)$$

For such a matrix we do not have a transition probability formula akin to (27), however, we may still use (25) to get a qualitative understanding of our results referred to this model.

III. SIMULATION AND RESULTS

For DUNE simulations, we will use the optimized beam as described in the CDR [70] and make use of the files from Ref. [76]. We use an exposure of 150 kt MW year exposure each for the neutrino and antineutrino channels. Both the neutrino mode (Forward Horn Current - FHC) and antineutrino mode (Reverse Horn Current - RHC) are used for 3.5 years on each. We are also using both the appearance ($\nu_\mu \rightarrow \nu_e$) and disappearance ($\nu_\mu \rightarrow \nu_\mu$) channels on neutrino and antineutrino modes. All NC and CC background rates discussed in detail in Ref. [70] Section 3.6.1 are included.

Throughout this section, we use the SO parameters from the global fit based on data available in January 2018 [77, 78] assuming normal ordering (NO) and some modifications. The ranges provided are not symmetric

What modifications?

Parameter	Value	Error
θ_{12}	33.62°	0.77°
θ_{23}	47.2°	2.9°
θ_{13}	8.54°	0.15°
$\frac{\Delta m_{31}^2}{10^{-5} \text{eV}^2}$	7.40	0.21
$\frac{\Delta m_{31}^2}{10^{-3} \text{eV}^2}$	2.494	0.032
δ	varies	-
ρ	2.97 g cm^{-3}	-
Baseline L	1300km	-

TABLE I: Relevant parameters assumed for our DUNE analysis.

about the fit values, but we will take them as symmetric by taking the average of the one-sided deviations. Due to the relatively unconstrained value of δ , we consider different values for this parameter with special emphasis on $\delta = -\pi/2$, which is rather similar to the current best-fit value. As such, no priors are assigned to δ . We summarize this information in Table I.

For all subsequent statistical analyses we will use the GLoBES package [79, 80], while oscillation probabilities are calculated using NuSQuIDS [81].

This study relies on the χ^2 test statistic to compare data generated by a set of “true” parameters ξ^{true} against a hypothesis that assumes a set of “test” values ξ . Unless otherwise stated, the parameters ξ^{true} will have the values in Table I. The values of δ and $\bar{\Gamma}$ will be provided on a case-by-case basis. In the context of DUNE and GLoBES, χ^2 is defined as

$$\chi^2(\xi, \xi^{\text{true}}) = \sum_i \frac{(N_i(\xi) - N_i(\xi^{\text{true}}))^2}{N_i(\xi^{\text{true}})} \quad (29)$$

where the N_i is the expected number of events in the i 'th energy bin. When including priors, GLoBES modifies χ^2 by adding an extra term

$$\chi^2 \rightarrow \chi^2 + \sum_j \frac{(\xi_j - \xi_j^{\text{true}})^2}{\sigma_j^2} \quad (30)$$

where the summation in j is over all parameters for which $\sigma_j \neq 0$. In this and all subsequent definitions for χ^2 , it is implicit that Γ and γ are used interchangeably depending on the assumed model.

A. Determination of standard oscillation parameters

Our first test consists on performing SO fits on data that includes decoherence. The data is generated assuming the true parameter values in Table I, for $\delta^{\text{true}} = -\pi/2$ and Γ^{true} and no priors. The test hypothesis is $\Gamma = 0$ and we obtain χ^2_{\min} by marginalizing over the SO parameters,

data \rightarrow an asimov sample is generated.

En reactores $\Gamma L \ll D_{\text{one}}$
y estos miden muy bien θ_{13} .
no alivia esto la confusión molecular por Γ ? 5

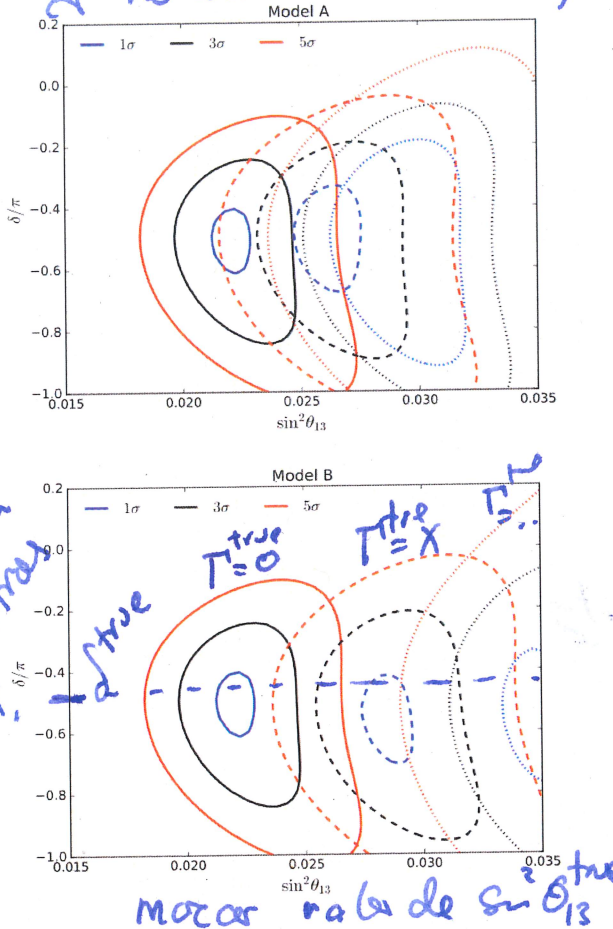


FIG. 1: Effects of decoherence on standard oscillation fits for $\delta^{\text{true}} = -\pi/2$. We show the $\Delta\chi^2$ contours or $\Gamma^{\text{true}} = 0$ GeV, 2×10^{-24} GeV and 5×10^{-24} GeV (solid, dashed, and dotted lines respectively).

attaining its minimum for a set of parameters which we label as “fit”. We project the χ^2 function on the $\theta_{13} - \delta$ plane

$$\Delta\chi^2 = \chi^2(\theta_{13}, \delta, \Gamma = 0, \delta^{\text{true}}, \Gamma^{\text{true}}) - \chi^2_{\min}(\theta_{13}^{\text{fit}}, \delta^{\text{fit}}, \Gamma = 0, \delta^{\text{true}}, \Gamma^{\text{true}}), \quad (31)$$

where all unmentioned test parameters are fixed to their fit values.

We plot our results in Fig. 1. As we increase the value of Γ^{true} , the SO fit shifts towards higher values of θ_{13} for both models. We can explain this behavior through Eq.(25) where: as long as we increase Γ the $\nu_\mu \rightarrow \nu_e$ transition probability grows in an energy-independent way, which, if it is fitted under the SO assumption, can be misconstrued as a larger mixing angle θ_{13} . Both plots have similar shapes, where model B has a more notable shift to higher θ_{13} ; a feature that is explained by looking at Eq. (25), where the parameters Γ_3, Γ_8 are non-zero

and increase the value of the shift.

On the other hand, the general shape of the contour plots remains the same. We also made the same analysis using the FHC and RHC separately, where the former provided stronger constraints compared to the latter, because of the higher statistics of the former. Similarly, we found that the appearance channels restrict the parameter space better than the disappearance channels.

B. Effects of decoherence on constraining δ *an asimov sample.*

To test the ability of DUNE to constrain decoherence parameters, we generate data assuming true values for δ and Γ and make a χ^2 plot on the δ, Γ plane. Our χ^2 in this case assumes δ and Γ as free parameters and all remaining parameters are fixed to their true-fit values (there is no marginalization here). Our findings are displayed in Fig. 2. *profiling.*

If data is generated assuming the pure SO scenario and maximal CP violation, then, when we fitted it taking decoherence as described by model A, we observe that, at $\delta \sim -\pi/2$, Γ is still compatible at the $1, 3, 5\sigma$ level with values similar to: 10^{-24} GeV, 6×10^{-24} GeV, and 9×10^{-24} GeV, respectively. When we look at model B, we appreciate that the constraints in Γ are more stringent with values similar to: 10^{-24} GeV, 2.7×10^{-24} GeV, and 4×10^{-24} GeV, for $1, 3, 5\sigma$, respectively, at $\delta \sim -\pi/2$. This ability to be more stringent than model A is, mostly, due to the increased contribution from the first order correction to the transition probability (see Eq. (25)). A noteworthy observation is that the width of the contour levels in δ is approximately the same between these two models.

By increasing Γ^{true} to 10^{-24} GeV, we can distinguish between pure oscillations and oscillations plus decoherence at the 1σ level, with δ being well constrained. The degeneracy behaviour in (Γ, δ) of these plots resembles the degeneracies in the CP asymmetries reported in our previous work [67], particularly with those corresponding to the low energy range of DUNE’s neutrino beams. We also pointed out in [67] that, for $\delta^{\text{true}} = -\pi/2$, we had similar asymmetries with $\delta = \pi/2$ and these could be confused at low energies. However, when taking the whole of DUNE’s energy range into account, we showed that no similarities remain. This prediction is consistent with our current results, since we found that none of the plots of Fig. 2 exhibit a secondary contour appearing in the vicinity of $\delta = \pi/2$.

C. Constraining the decoherence parameter

For this study the simulated data assumes $\Gamma^{\text{true}} = 0$ and a fit is performed for a given test parameter Γ . Our test statistic is

$$\chi^2(\Gamma) = \chi^2(\Gamma, \delta^{\text{true}}, \Gamma^{\text{true}} = 0) \quad (32)$$

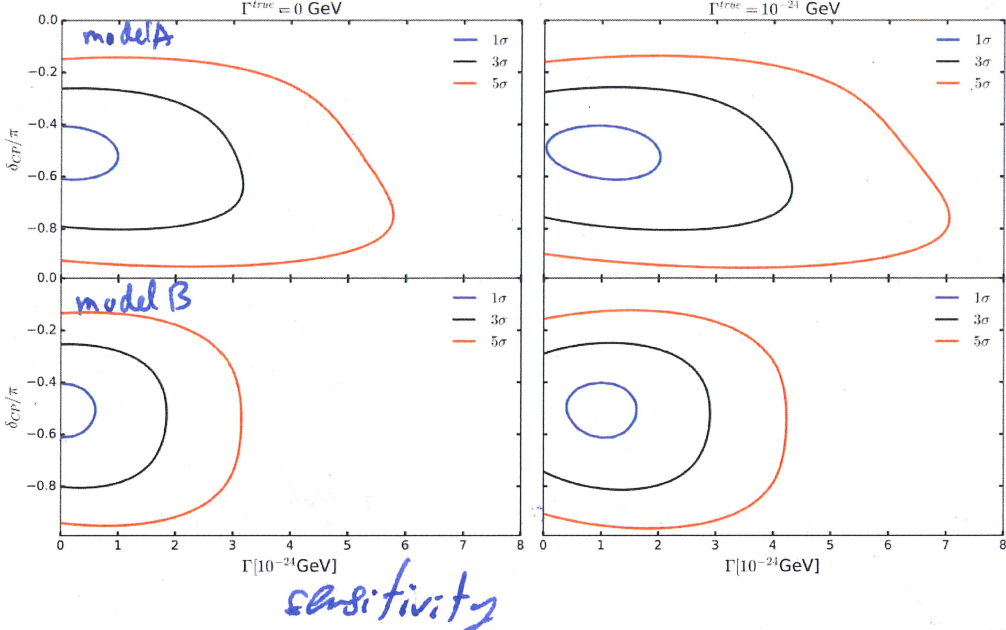


FIG. 2: Left(right) panels: DUNE's ability to constrain decoherence parameters, for $\Gamma^{\text{true}} = 0 \text{ GeV}$ (10^{-24} GeV). The top(bottom) panels assume model A(B).

where we marginalize over all standard oscillation parameters. We show the results in Fig. 3. The sensitivity to $\Gamma/(10^{-24}\text{GeV})$ for the model A is in the range 1.5-2.1, 5.4-6.7 and 8.2-10.3 at the 1σ , 3σ and 5σ levels. On the other hand, the mode of the invariant matrix, model B, has a sensitivity almost invariant in δ and it is stronger than one predicted for model A, as we have already seen it in Fig. 2. This is a result of the increased contribution from the first order decoherence term for model B, which does not depend on the CP phase; the effect of other δ -dependent terms in a perturbative expansion are suppressed, such as the $\Gamma\theta_{13}$ term present in Eq. (27).

For either model, DUNE's sensitivity to Γ is superior to the previously reported KamLAND's 95% C.L. sensitivity of $6.8 \times 10^{-22} \text{ GeV}$ [56] and the 90% C.L. sensitivity of $1.2 \times 10^{-23} \text{ GeV}$ [68]. Our current results are of the same order of magnitude as those reported in a recent IceCube study [69]. We do remark that the decoherence models used in these previous studies are slightly different than ours and act as benchmarks.

*max T₃₅ : DUNE
T (exposure)
create event
in memory
plot several
sener extra
discussions
on in griffo.*

D. Mass ordering sensitivity

Mass ordering sensitivity is obtained by comparing generated data from an NO assumption with decoherence against an IO hypothesis without decoherence. When generating data, a value of Γ^{true} is assumed and the test statistic is marginalized in all oscillation parameters

The a prior set. profiled

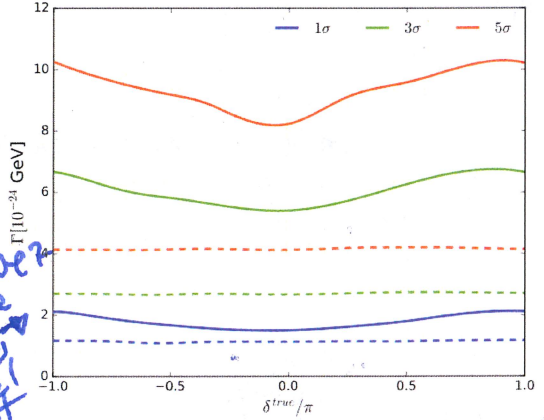


FIG. 3: Sensitivity to the decoherence parameter Γ , as a function of δ^{true} , for different confidence levels. Solid lines correspond to model A and dashed lines correspond to model B.

while keeping $\Gamma = 0$ fixed, meaning that

$$\chi^2_{\text{MO}} = \chi^2(\Delta m_{31}^2 < 0, \Gamma = 0, \Delta m_{31}^{2\text{true}} > 0, \delta^{\text{true}}, \Gamma^{\text{true}}) . \quad (33)$$

The sensitivities are presented in Fig. 4 for different Γ^{true} . We see that, regardless of δ^{true} and our assumed decoherence model, the sensitivity is well above 5σ for our chosen values of the decoherence parameter and in fact improves it. To explain this feature, we point out that

the IO fit yielded similar values for the SO parameters for all δ^{true} , with the fit value δ^{fit} in the vicinity of $\delta = -\pi/2$. This occurred for all the Γ^{true} that we analyzed. When we studied the IO fit, we noticed that the probability in the $\nu_\mu \rightarrow \nu_e$ channel is lower, and well separated, than that corresponding to the NO data in the energy range 2 GeV-4 GeV. Being that, as long as Γ^{true} increases, the NO transition probabilities do as well. In return, the resulting IO fit transition probabilities separate more and more from the corresponding NO assumptions from the data. This separation leads to the observed increase in sensitivity. The impact of Γ on the sensitivity is strongest as we approach $\delta^{\text{true}} = \pi/2$.

E. CP violation sensitivity

To obtain DUNE's sensitivity to CP violation, we adopt a definition similar to the one presented in [70]

$$\chi_{CP}^2 = \min[\chi^2(\delta = 0, \Gamma = 0, \delta^{\text{true}}, \Gamma^{\text{true}}), \chi^2(\delta = \pi, \Gamma = 0, \delta^{\text{true}}, \Gamma^{\text{true}})] \quad (34)$$

and we marginalize over all unmentioned test parameters. We checked that, after ~~marginalizing~~^{profile}, the oscillation parameters remain approximately the same, with the exception of θ_{13} that settles at higher values to account for the increased event rates in the appearance channels due to decoherence. The IO alternative was never preferred during the minimization procedure of χ^2 . This observation is easily explained by Fig. 4 because DUNE can distinguish between the hierarchies with a large significance.

The data generated using NO has an additional fake CP violation contribution coming from the matter potential present in the term proportional to $\Gamma\theta_{13}$, which is mistaken in an SO fit as CP violation. For this reason, even when $\delta^{\text{true}} = 0, \pi$, decoherence may cause us to reject the null hypothesis (no CP violation). Due to this decoherence induced CP violation, decoherence lets us reject the null hypothesis at a higher confidence level throughout all values of δ .

IV. SUMMARY AND CONCLUSIONS

We have tackled diverse aspects of the decoherence phenomenon in the context of neutrino oscillations. From the theoretical side, we derived a general expression for invariant decoherence matrices that are diagonal (under rotations from VMB to MMB). The advantage of this type of matrix is its simple implementation into the matter oscillation probabilities formula as clarified in [67]. On the other hand, we have probed an invariant and non-invariant decoherence matrices under realistic circumstances within a DUNE simulated environment. We have achieved a sensitivity for the decoherence parameter of $\mathcal{O}(10^{-24} \text{ GeV})$ at 3σ and for $\delta = -\pi/2$, in the

estimated

best-case scenario (the invariant matrix model). A very interesting result is the presence of the degeneracy between Γ and δ , predicted at the theoretical level in [67]: depending on the value of the decoherence parameter, it becomes difficult to disentangle the scenarios where the data contains decoherence or not. Additionally, we have observed that, if decoherence plus standard oscillation is embodied within the data, the pure standard oscillation fit tends to select higher values of $\sin^2 \theta_{13}$ compared to the pure oscillation case. Finally, we have also seen that the decoherence phenomenon mildly affects the DUNE sensitivity on the mass hierarchy, while the CP sensitivity is clearly improved but with the disadvantage that even a true lack of CP violation ($\delta^{\text{true}} = 0, \pi$) can be confused with CP violation.

? Parece
que no hay
7
7
bar.
may
interplay!

V. ACKNOWLEDGEMENTS

The authors acknowledge funding by the Dirección de Gestión de la Investigación at PUCP, through grant DGI-2017-3-0019. They would also like to thank F. de Zela, J. Jones-Pérez and C. Argüelles for useful discussions and a very careful reading of the manuscript.

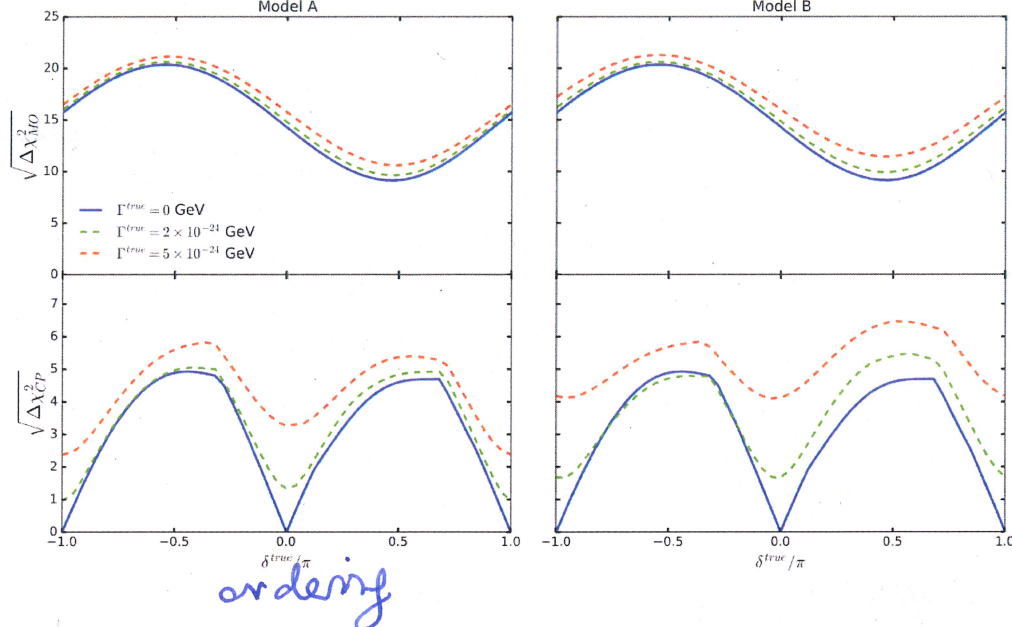


FIG. 4: Mass Hierarchy and CP violation sensitivity for our decoherence matrix models.

APPENDIX A: ROTATION MATRICES

We use the following forms of the unitary operators U_{ij}

$$\begin{aligned} U_{23} &= \begin{pmatrix} 1 & 0 & 0 \\ 0 & \cos \theta_{23} & \sin \theta_{23} \\ 0 & -\sin \theta_{23} & \cos \theta_{23} \end{pmatrix} \\ U_{13} &= \begin{pmatrix} \cos \theta_{13} & 0 & \sin \theta_{13} \\ 0 & 1 & 0 \\ -\sin \theta_{13} & 0 & \cos \theta_{13} \end{pmatrix} \\ U_{12} &= \begin{pmatrix} \cos \theta_{12} & \sin \theta_{12} & 0 \\ -\sin \theta_{12} & \cos \theta_{12} & 0 \\ 0 & 0 & 1 \end{pmatrix} \end{aligned} \quad (\text{A1})$$

The elements of P are defined as follows:

$$P_{ij}(\delta, \phi_1, \phi_2) = 2\text{Tr} \left[U_T^\dagger(\delta, \phi_1, \phi_2) F_i U_T(\delta, \phi_1, \phi_2) F_j \right] \quad (\text{B2})$$

Now replacing $U_T(\delta, \phi_1, \phi_2) = U_\delta^\dagger U_T(0, 0, 0) U_\phi^\dagger(\phi_1, \phi_2)$ in the above equation, we obtain

$$P(\delta, \phi_1, \phi_2) = S^T(\delta) P(0, 0, 0) \hat{S}^T(\phi_1, \phi_2) \quad (\text{B3})$$

where S, \hat{S} are written in block-diagonal form

$$S(\delta) = \begin{pmatrix} \mathbb{I}_{3 \times 3} & & \\ & R(\delta) & \\ & & R(\delta) \\ & & & 1 \end{pmatrix} \quad (\text{B4})$$

APPENDIX B: DEFINITIONS OF P , $R(\delta)$ AND $\hat{R}(\phi)$

We define the two-dimensional rotation matrix $R(\theta)$ by

$$R(\theta) = \begin{pmatrix} \cos \theta & \sin \theta \\ -\sin \theta & \cos \theta \end{pmatrix} \quad (\text{B1})$$

$$\hat{S}(\phi_1, \phi_2) = \begin{pmatrix} R(\phi_1) & & & \\ & 1 & & \\ & & R(\phi_2) & \\ & & & R(\phi_2 - \phi_1) \\ & & & & 1 \end{pmatrix} \quad (\text{B5})$$

[1] S. Fukuda et al. (Super-Kamiokande Collaboration), Phys. Rev. Lett. **86**, 5651 (2001).

[2] Q.R. Ahmad et al. (SNO Collaboration), Phys. Rev. Lett. **89**, 011302 (2002).

- [3] Y. Fukuda et al. (Super-Kamiokande Collaboration), Phys. Rev. Lett. **81**, 1562 (1998).
- [4] T. Kajita et al. (Super-Kamiokande Collaboration), Nucl. Phys. B **908**, 14 (2016).
- [5] T. Araki et al. (KamLAND Collaboration), Phys. Rev. Lett. **94**, 081801 (2005).
- [6] F.P. An et al. (Daya Bay Collaboration), Phys. Rev. Lett. **108**, 171803 (2012).
- [7] P. Adamson et al. (MINOS Collaboration), Phys. Rev. D **77**, 072002 (2008).
- [8] J. M. Berryman, A. de Gouv  a, D. Hernandez and R. L. N. Oliveira, Phys. Lett. B **742**, 74 (2015).
- [9] J. A. Frieman, H. E. Haber and K. Freese, Phys. Lett. B **200**, 115 (1988).
- [10] R. Raghavan, X.-G. He and S. Pakvasa, Phys. Rev. D **38**, 1317 (1988).
- [11] Z. Berezhiani, G. Fiorentini, M. Moretti and A. Rossi, Z. Phys. C **54**, 581 (1992).
- [12] Z. Berezhiani, G. Fiorentini, A. Rossi and M. Moretti, JETP Lett. **55**, 151 (1992).
- [13] Z. G. Berezhiani and A. Rossi, arXiv:hep-ph/9306278.
- [14] V. D. Barger et al., Phys. Lett. B **462**, 109 (1999).
- [15] J. F. Beacom and N. F. Bell, Phys. Rev. D **65**, 113009 (2002).
- [16] A. S. Joshipura, E. Masso and S. Mohanty, Phys. Rev. D **66**, 113008 (2002).
- [17] A. Bandyopadhyay, S. Choubey and S. Goswami, Phys. Lett. B **555**, 33 (2003).
- [18] S. Ando, Phys. Rev. D **70**, 033004 (2004).
- [19] G. Fogli, E. Lisi, A. Mirizzi and D. Montanino, Phys. Rev. D **70**, 013001 (2004).
- [20] S. Palomares-Ruiz, S. Pascoli and T. Schwetz, JHEP **0509**, 048 (2005).
- [21] M. C. Gonzalez-Garcia and M. Maltoni, Phys. Lett. B **663**, 405 (2008).
- [22] M. Maltoni and W. Winter, JHEP0807, 064 (2008).
- [23] P. Baerwald, M. Bustamante and W. Winter, JCAP **1210**, 020 (2012).
- [24] D. Meloni and T. Ohlsson, Phys. Rev. D **75**, 125017 (2007).
- [25] C.R. Das and J. Pulido, Phys. Rev. D **83**, 053009 (2011).
- [26] L. Dorame, O.G. Miranda and J.W.F. Valle, Front. in Phys. **1**, 25 (2013).
- [27] R.A. Gomes, A.L.G. Gomes and O.L.G. Peres, Phys. Lett. B **740**, 345 (2015).
- [28] R. Picoreti, M.M. Guzzo, P.C. de Holanda and R.L.N. Oliveira, Phys. Lett B **761**, 70 (2016).
- [29] T. Abrah  o, H. Minakata and A.A. Quiroga, JHEP **11**, 001 (2015).
- [30] M. Bustamante, J.F. Beacom and K. Murase, Phys. Rev. D **95**, 063013 (2017).
- [31] A.M. Gago, R.A. Gomes, A.L.G. Gomes, J. Jones-Perez and O.L.G. Peres (2017). arXiv:1705.03074.
- [32] P. Coloma and O.L.G. Peres (2017). arXiv: 1705.03599
- [33] M. V. Ascencio-Sosa, A. M. Calatayud-Cadenillas, A. M. Gago and J. Jones-Prez, Eur. Phys. J. C **78**, no. 10, 809 (2018)
- [34] M. C. Gonzales-Garcia, M. M. Guzzo, P. Krastev and H. Nunokawa, Phys. Rev. Lett. **82**, 3202 (1999).
- [35] S. Bergmann, M. M. Guzzo, P. C. de Holanda, P. Krastev and H. Nunokawa, Phys. Rev. D **62**, 073001 (2000).
- [36] M. M. Guzzo, P. C. de Holanda and O. L. G. Peres, Phys. Lett. B **591**, 1 (2004).
- [37] A. M. Gago, M. M. Guzzo, H. Nunokawa, W. J. C. Teves and R. Zukanovich Funchal, Phys Rev D **64**, 073003 (2001).
- [38] A. M. Gago et al., Phys. Rev. D **65**, 073012 (2002).
- [39] T. Ohlsson, Rept. Prog. Phys. **76**, 044201 (2013).
- [40] A. Esmaili and A. Y. Smirnov, JHEP **1306**, 026 (2013).
- [41] D. Colladay and V. A. Kostelecky, Phys. Rev. D **55**, 6760 (1997).
- [42] S. R. Coleman and S. L. Glashow, Phys. Rev. D **59**, 116008 (1999).
- [43] S. R. Coleman and S. L. Glashow, Phys. Lett. B **405**, 249 (1997).
- [44] D. Colladay and V. A. Kostelecky, Phys. Rev. D **58**, 116002(1998).
- [45] P. Adamson *et al.* [MINOS Collaboration], Phys. Rev. Lett. **105**, 151601 (2010)
- [46] A. A. Aguilar-Arevalo *et al.* [MiniBooNE Collaboration], Phys. Lett. B **718**, 1303 (2013).
- [47] Y. F. Li and Z. h. Zhao, Phys. Rev. D **90**, no. 11, 113014 (2014).
- [48] J. Ellis, N. E. Mavromatos and D. V. Nanopoulos, Phys. Lett. **B293**, 37 (1992); Int. J. Mod. Phys. A**11**, 1489 (1996).
- [49] F. Benatti and R. Floreanini, Ann. of Phys. **273**, 58 (1999).
- [50] S. Hawking, Comm. Math. Phys. **87**, 395 (1983); Phys. Rev. D **37**, 904 (1988); Phys. Rev. D **53**, 3099 (1996); S. Hawking and C. Hunter, Phys. Rev. D **59**, 044025 (1999).
- [51] F. Benatti and R. Floreanini, JHEP0002, 32 (2000).
- [52] F. Benatti and R. Floreanini, Phys. Rev. D **64**, 085015 (2001).
- [53] A.M. Gago, E.M. Santos, W.J.C. Teves and R. Zukanovich Funchal, arXiv:0208166.
- [54] R.L.N. Oliveira and M.M. Guzzo, Eur. Phys. J. C **69**, 493 (2010).
- [55] R.L.N. Oliveira and M.M. Guzzo, Eur. Phys. J. C **73**, 2434 (2013).
- [56] R.L.N Oliveira, Eur. Phys. J. C **76**, 417 (2016).
- [57] E. Lisi, A. Marrone and D. Montanino, Phys. Rev. Lett. **85**, 1166 (2000).
- [58] Y. Farzan, T. Schwetz and A.Y. Smirnov, JHEP0807, 067 (2008).
- [59] G. Barenboim and E.N. Mavromatos, JHEP01, 31 (2005).
- [60] P. Bakhti, Y. Farzan and T. Schwetz, JHEP05, 007 (2015).
- [61] A.M. Gago, E.M. Santos, W.J.C. Teves and R. Zukanovich Funchal, Phys. Rev. D **63**, 073001 (2001).
- [62] D. Morgan, E. Winstanley, J. Brunner and L. F. Thompson, Astropart. Phys. **25**, 311 (2006).
- [63] G. L. Fogli, E. Lisi, A. Marrone, D. Montanino and A. Palazzo, Phys. Rev. D **76**, 033006 (2007).
- [64] R. L. N. Oliveira, M. M. Guzzo, and P. C. de Holanda, Phys. Rev. D **89**, 053002 (2014).
- [65] G. Balieiro Gomes, M. M. Guzzo, P. C. de Holanda and R. L. N. Oliveira, Phys. Rev. D **95**, 113005 (2016).
- [66] M.M. Guzzo, P.C. de Holanda and R.L.N. Oliveira, Nucl. Phys. B **908**, 408 (2016).
- [67] J.A. Carpio, E. Massoni and A.M. Gago, Phys. Rev. D **97**, 115017 (2018).
- [68] G. Balieiro Gomes, D. V. Forero, M. M. Guzzo, P. C. De Holanda and R. L. N. Oliveira, arXiv:1805.09818.
- [69] P. Coloma, J. Lopez-Pavon, I. Martinez-Soler and H. Nunokawa, Eur. Phys. J. C **78**, 614 (2018).
- [70] R. Acciari *et al.* [DUNE Collaboration],